Fractal-like tree networks increasing the permeability

Jun Chen, Boming Yu,* Peng Xu, and Yonghua Li
Department of Physics, Huazhong University of Science and Technology, 1037 Luoyu Road, Wuhan 430074, People's Republic of China

(Received 2 November 2006; published 1 May 2007)

The effective permeability of composites embedded with self-similar fractal-like tree networks is studied. The effective permeability tensor of the composites is derived and is found to be related to microstructures of the networks. The present results show that the larger the ratio of successive branching channel diameters, the higher the effective permeability; the higher the relative surface porosity of the tree networks and matrix, the higher the effective permeability; the denser the tree networks, the lower the effective permeability; the longer the branches, the lower the effective permeability. It is found that the dimensionless effective permeability of composites scales as the diameter exponent by $K_{e,y}^{+} \sim \beta^{\alpha m}$, with $\alpha \approx 4$. It is also found that when $m > 1$ and $n\beta^4/\gamma < 1$, the effective permeability $K_{e,y}^{+}$ scales as the iteration m, $\ln K_{e,y}^{+}/m \sim \ln(n\beta^4/\gamma)$. The fractal-like tree networks can significantly increase the effective permeability of the composites compared to the traditional parallel nets under properly chosen structural parameters.

DOI: 10.1103/PhysRevE.75.056301 PACS number(s): 47.56.+r, 64.60.Ak

I. INTRODUCTION

Recently, increased attention has been focused on the tree networks because of their wide existence in nature such as lungs, vasculatures, botanical trees, river basins, porous networks in oil-water reservoirs and their relevance to many real systems [1–9], and applications such as the world wide web, the internet, social and energy transport networks [10–12]. It has been shown that natural tree network systems often give the minimal resistance and optimal vascular diameter for driving the blood in mammals and water in plants. These mechanisms are recently applied in design of energy transport systems and cooling systems of electronic chips due to increasing miniaturization of chips in microelectronic equipments and the production of redundant heat.

Bejan [13–15] developed a solution to the fundamental problem of how to design a flow path with minimum overall resistance between one point and many points situated equidistantly on a line or circle centered at the point. The solution was obtained by a sequence of optimization and organization steps. It was shown that in an optimal design the flow path forms a tree-shaped network. Bejan called this approach a constructal theory, and emphasized the robustness of optimized tree-shaped flows. Neagu and Bejan [16] showed that the global thermal resistance between a volume and one point could be reduced to unprecedented levels by shaping the external boundary of each volume element. The resulting architecture is a leaflike tree structure with high-conductivity nerves and low-conductivity leaves. Bejan *et al.* [17] investigated the flow systems consisting of T- and Y-shaped assemblies of ducts, channels, and crosses, and achieved the optimum thermodynamic performance by minimizing the overall flow resistance encountered over a finite-size territory. Wechsatol *et al.* [18] utilized the constructal method to investigate the optimal tree-shaped networks for fluid flow in a disc-shaped body. Yu and Li [19] also used the constructal method and principle to analyze the thermal conductivity of fractal-like tree networks. The results indicate that the thermal conductivity of the tree network itself may be less than that of the original material by several orders of magnitude, and fractal-like tree networks can significantly reduce the thermal conductivity compared to an equivalent single cylinder. Xu *et al.* [20,21] systematically investigated the effective permeability of the fractal-like tree branched networks between one point and a straight line, one point and a disc-shaped area.

In this paper, we study the effective permeability of composites with embedded self-similar V-shaped fractal-like tree channel networks based on the constructal theory. This study is different from previous works [17,18,20,21] because matrix material is assumed to be permeable. We attempt to obtain the analytic expression of the effective permeability tensor of the composites. The results might find applications in design of composites (such as space shuttle equipment) with higher permeability, in oil recovery, and in cooling of electronic chips and/or components.

II. EFFECTIVE PERMEABILITY OF COMPOSITES WITH EMBEDDED FRACTAL-LIKE TREE NETWORKS

A. Permeability of the fractal-like tree networks

For simplicity in this analysis, we start with the V-shaped structure, a possible smallest dichotomous structure. Figure 1 shows the channel-matrix system with different branching levels. Suppose a finite number of elements shaped as V start to grow from the bottom of a matrix. These V-shaped assemblies are assumed to have a fixed area (volume), length ratio, and branching angle. With the network channel increasing, the branching channels become more and more slender. If the stems are assumed to be infinitely thin, the V-shaped network structures as shown in Fig. 1 are fractals [22]. Since there is a possible smallest element or unit structure that the daughter branches may touch each other after finite repeats,

*Author to whom correspondence should be addressed. Electronic address: yuboming2003@yahoo.com.cn

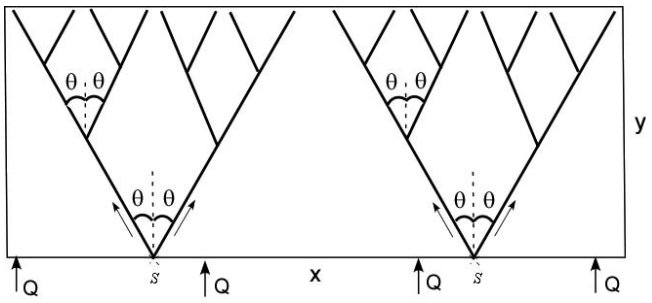

(a)

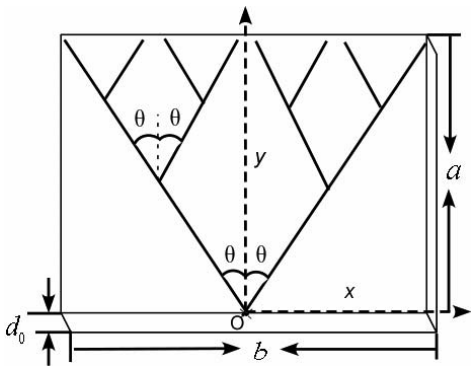

(b)

FIG. 1. (a) Schematic of composite with embedded fractal-like tree networks, with fluid flowing into both matrix and networks, and (b) a unit of the permeable matrix with an embedded V-shaped fractal-like tree network.

the branch volume and branching angle are restricted to avoid touching each other of the daughter branches. As shown in Fig. 1(b), $\tan\theta = b/(2a)$, the opening or branching angle θ is in the range of $0-\pi/2$ and is closely related to the length and width of the matrix unit. Therefore, the branching tree networks in this paper are called the fractal-like tree networks.

We assume that the permeable matrix has a permeability K_m and the networks are embedded in the matrix, and the channel walls of the networks are also permeable. The rate flowing into the channel walls is equal to that flowing out of the channel walls, so that the flow rates in the matrix and inside the channels of the network do not interfere with each other due to flow continuity. This implies that there is no net contribution to the local flux through the walls. This assumption is just for simplicity of analysis. An accurate analysis of local flow flux through the permeable channel walls may need to solve the Stokes equation for flow in channels and the Brinkman equation for flow in matrix and will be addressed elsewhere. Figure 1(b) shows a V-shaped fractal-like tree network embedded in matrix of width a, length b, and thickness d_0, and the Cartesian coordinate system is shown in Fig. 1(b). We assume that one-dimensional steady state and laminar incompressible fluid flow into the composite along the y direction [see Fig. 1(a)]. Due to symmetry, we only analyze the permeabilities in the positive x and y directions, separately.

In order to derive the effective permeability of the composite, we first derive the permeability of the V-shaped

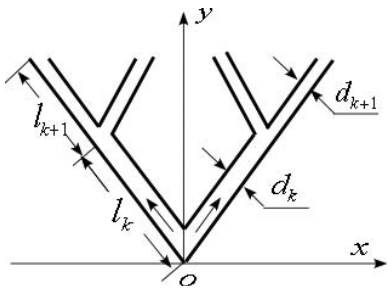

FIG. 2. A typical structure of the "V-shaped" fractal-like tree network at the kth level.

fractal-like tree network channels. We assume that each branch of the network is a smooth cylinder or channel. Figure 2 shows a typical structure of the "V-shaped" fractal-like tree network at some intermediate level k, where d_k and l_k are the channel diameter and channel length of the kth level ($k=0,1,2,\ldots$), respectively. The case of $k=0$ represents an initial V-shaped structure, and each cylinder branches into n ($=2$ is used in this work). We define $\gamma = l_{k+1}/l_k$, the ratio of length of the channel at the $(k+1)$th branching level to that at the kth branching level, and therefore, we have $l_k = l_0\gamma^k$. Note that the fractal dimension D is generated from $n=\gamma^{-D}$ [22]. So in Fig. 1(a) $\gamma=0.674$, then $D=1.74$; in Fig. 1(b) $\gamma=0.622$, which results in $D=1.46$.

For the fractal-like tree networks and according to the Darcy law, we have

$$K_x = \frac{Q_x \mu b}{2A_x \Delta p_x}, \tag{1a}$$

$$K_y = \frac{Q_y \mu a}{A_y \Delta p_y}, \tag{1b}$$

where Q, A, K, Δp, and μ are, respectively, the flow rate, cross-sectional area of the networks, permeability, pressure drop across the networks and the dynamic viscosity of fluid. The subscripts x and y in Eq. (1) represent the corresponding parameters along the positive x and y directions, respectively.

The pressure drops Δp_x and Δp_y in Eq. (1) can be expressed as

$$\Delta p_x = \Delta p \sin\theta, \tag{2a}$$

$$\Delta p_y = \Delta p \cos\theta, \tag{2b}$$

where $\Delta p = \Sigma_{k=0}^{m} \Delta p_k$ is the total pressure drop across the network, and Δp_k is the pressure drop across the kth level network channel, m ($m=0,1,2,\ldots$) is the total number of levels of the network. According to Hagen-Poiseuille equation, Δp_k is expressed as

$$\Delta p_k = \frac{128\mu}{\pi}\frac{l_k Q_k}{d_k^4}, \tag{3}$$

where Q_k is the flow rate in the kth level branching channel. Then, due to Eq. (3), Eq. (2) can be rewritten as

$$\Delta p_x = \frac{128\mu \sin\theta}{\pi}\sum_{k=0}^{m}\frac{l_k Q_k}{d_k^4}, \tag{4a}$$

$$\Delta p_y = \frac{128\mu \cos\theta}{\pi}\sum_{k=0}^{m}\frac{l_k Q_k}{d_k^4}. \tag{4b}$$

The flow rates Q_x and Q_y can be written as

$$Q_x = n^k Q_k \sin\theta, \tag{5a}$$

$$Q_y = n^{k+1} Q_k \cos\theta. \tag{5b}$$

Substituting Eq. (5) into Eq. (4) yields

$$\Delta p_x = \frac{128\mu Q_x}{\pi}\sum_{k=0}^{m}\frac{l_k}{n^k d_k^4}, \tag{6a}$$

$$\Delta p_y = \frac{128\mu Q_y}{n\pi}\sum_{k=0}^{m}\frac{l_k}{n^k d_k^4}. \tag{6b}$$

Inserting Eq. (6) into Eq. (1) yields

$$K_x = \frac{\pi(b/2)}{128A_x}\frac{1}{\sum_{k=0}^{m}\frac{l_k}{n^k d_k^4}}, \tag{7a}$$

$$K_y = \frac{n\pi a}{128A_y}\frac{1}{\sum_{k=0}^{m}\frac{l_k}{n^k d_k^4}}, \tag{7b}$$

where the cross-sectional area $A_x = ad_0$ and $A_y = bd_0$, see Fig. 1(b), and d_0 is the diameter of the initial branching level 0, which is equal to the thickness of the matrix. The length and width of the matrix change with the branching levels m and satisfy

$$a = \sum_{k=0}^{m} l_k \cos\theta, \tag{8a}$$

$$b = \sum_{k=0}^{m} 2l_k \sin\theta. \tag{8b}$$

Substituting Eq. (8) into Eq. (7), we get the permeability of the fractal-like tree network,

$$K_x = \frac{\pi d_0^3}{128 l_0}\frac{1-\gamma/(n\beta^4)\tan\theta}{1-[\gamma/(n\beta^4)]^{m+1}}, \tag{9a}$$

$$K_y = \frac{\pi d_0^3}{128 l_0}\frac{1-\gamma/(n\beta^4)}{1-[\gamma/(n\beta^4)]^{m+1}}\frac{n}{2\tan\theta}, \tag{9b}$$

where the scale factor $\beta = d_{k+1}/d_k$. Since the factor $\pi d_0^3/(128 l_0)$ in Eq. (9) is a constant and has the dimension of permeability, we thus obtain the dimensionless permeability of the network,

$$K_x^+ = \frac{K_x}{\pi d_0^3/(128 l_0)} = \tan\theta\frac{1-\gamma/(n\beta^4)}{1-[\gamma/(n\beta^4)]^{m+1}}, \tag{10a}$$

$$K_y^+ = \frac{K_y}{\pi d_0^3/(128 l_0)} = \frac{n}{2\tan\theta}\frac{1-\gamma/(n\beta^4)}{1-[\gamma/(n\beta^4)]^{m+1}}. \tag{10b}$$

It is clear that K_x^+ is equal to K_y^+ as $\theta=\pi/4$ in Eq. (10), and this is expected. Equation (10) also indicates that K_x^+ increases with the increase of the branching angle θ, while K_y^+ decreases at the same condition. These are reasonable because when θ increases, the branching channel will incline toward the positive x direction.

B. Effective permeability of composites with embedded fractal-like tree networks

Now we have obtained the permeability of the networks. In this section, we will derive the effective permeability K_e of composites with embedded fractal-like tree networks.

For an anisotropic saturated porous medium, the permeability tensor $\vec{K}_e$ is expressed as [23,24]

$$\vec{K}_e = \begin{bmatrix} K_{e,x} & 0 \\ 0 & K_{e,y} \end{bmatrix}, \tag{11}$$

where $K_{e,x}(K_{e,y})$ is the effective permeability of the composite in the positive $x(y)$ direction, which is also called the principal permeability in the principal direction. Note that in the above tensor, the off-diagonal elements are zero because the axes used in the calculation are assumed to be oriented along the principal directions.

Applying Darcy's law to the composite, we write the permeabilities as

$$K_{e,x} = \frac{Q_{e,x}\mu b}{2A_{e,x}\Delta p_{e,x}}, \tag{12a}$$

$$K_{e,y} = \frac{Q_{e,y}\mu a}{A_{e,y}\Delta p_{e,y}}, \tag{12b}$$

where $Q_{e,x}(Q_{e,y})$ is the total flow rate through the composite in the positive $x(y)$ direction, $A_{e,x}(A_{e,y})$ is the cross-sectional area of the composite in the $x(y)$ direction, and $\Delta p_{e,x}(\Delta p_{e,y})$ is the total pressure drop across the composite in the positive $x(y)$ direction. Equation (12) divided by Eq. (1) results in

$$\frac{K_{e,x}}{K_x} = \frac{Q_{e,x}}{Q_x}\frac{A_x \Delta p_x}{A_{e,x}\Delta p_{e,x}}, \tag{13a}$$

$$\frac{K_{e,y}}{K_y} = \frac{Q_{e,y}}{Q_y}\frac{A_y \Delta p_y}{A_{e,y}\Delta p_{e,y}}. \tag{13b}$$

Yu and Lee [25] solved the Stokes equation for flow in channels and the Brinkman equation in the region outside the channels for permeability of porous fabrics by assuming that the pressure drop along the channels is equal to that along the medium outside channels. Therefore, this work also assumes that $\Delta p_x = \Delta p_{e,x}$ and $\Delta p_y = \Delta p_{e,y}$, and due to $A_x = A_{e,x}$, $A_y = A_{e,y}$ and $\Delta p_x = \Delta p_{e,x}$, $\Delta p_y = \Delta p_{e,y}$, Eq. (13) can be reduced to

$$\frac{K_{e,x}}{K_x} = \frac{Q_{e,x}}{Q_x}, \tag{14a}$$

$$\frac{K_{e,y}}{K_y} = \frac{Q_{e,y}}{Q_y}. \tag{14b}$$

Equation (14) suggests that the ratios of $K_{e,x}/K_x$ and $K_{e,y}/K_y$ are exactly equal to those of $Q_{e,x}/Q_x$ and $Q_{e,y}/Q_y$, respectively. However, the flow rate is directly proportional to the cross-sectional area when flow velocity is assumed to be constant. Thus, we have

$$\frac{K_{e,x}}{K_x} = \frac{Q_{e,x}}{Q_x} = \frac{\Delta A_{V,ex}}{\Delta A_{V,x}} = 1 + \frac{\Delta A_{V,mx}}{\Delta A_{V,x}}, \tag{15a}$$

$$\frac{K_{e,y}}{K_y} = \frac{Q_{e,y}}{Q_y} = \frac{\Delta A_{V,ey}}{\Delta A_{V,y}} = 1 + \frac{\Delta A_{V,my}}{\Delta A_{V,y}}, \tag{15b}$$

where $\Delta A_{V,ex}(\Delta A_{V,ey})$ is the cross-sectional area of the pore spaces that the composite contains in the $x(y)$ direction, which contains the cross-sectional area $\Delta A_{V,mx}(\Delta A_{V,my})$ of the matrix pore spaces and the cross-sectional area $\Delta A_{V,x}(\Delta A_{V,y})$ of the branching channels in the $x(y)$ direction, i.e., $\Delta A_{V,ex}=\Delta A_{V,x}+\Delta A_{V,mx}$ and $\Delta A_{V,ey}=\Delta A_{V,y}+\Delta A_{V,my}$.

In order to establish the relation between the cross-sectional area of the matrix pore spaces and that of the branching channels, we introduce $\phi_{m,x}(\phi_{m,y})$ to represent the surface porosity of the matrix material in the $x(y)$ direction, and $\phi_x(\phi_y)$ the surface porosity of the branching channels of the networks in the $x(y)$ direction. Note that in general $\phi_{m,x} \neq \phi_{m,y}$ and $\phi_x \neq \phi_y$. Thus, we can get

$$\phi_{m,x} = \frac{\Delta A_{V,mx}}{A_{e,x}}, \quad \phi_{m,y} = \frac{\Delta A_{V,my}}{A_{e,y}}, \tag{16a}$$

$$\phi_x = \frac{\Delta A_{V,x}}{A_x}, \quad \phi_y = \frac{\Delta A_{V,y}}{A_y}. \tag{16b}$$

Inserting Eq. (16) into Eq. (15) and with the aid of $A_x=A_{e,x}$ and $A_y=A_{e,y}$, we obtain

$$\frac{K_{e,x}}{K_x} = 1 + \frac{\phi_{m,x}}{\phi_x}, \tag{17a}$$

$$\frac{K_{e,y}}{K_y} = 1 + \frac{\phi_{m,y}}{\phi_y}. \tag{17b}$$

Defining $\psi_x=\frac{\phi_{m,x}}{\phi_x}$ $\left(\psi_y=\frac{\phi_{m,y}}{\phi_y}\right)$ as the relative surface porosity of the matrix material with respect to the fractal-like tree networks in the x (y) direction, Eq. (17) can be expressed as

$$\frac{K_{e,x}}{K_x} = 1 + \psi_x, \tag{18a}$$

$$\frac{K_{e,y}}{K_y} = 1 + \psi_y. \tag{18b}$$

Substituting Eq. (9) into Eq. (18) yields the effective permeability $K_{e,x}$ and $K_{e,y}$,

$$K_{e,x} = \frac{\pi d_0^3 (1+\psi_x)\tan\theta}{128 l_0} \frac{1-\gamma/(n\beta^4)}{1-[\gamma/(n\beta^4)]^{m+1}}, \tag{19a}$$

$$K_{e,y} = \frac{\pi d_0^3}{128 l_0} \frac{(1+\psi_y)n}{2\tan\theta} \frac{1-\gamma/(n\beta^4)}{1-[\gamma/(n\beta^4)]^{m+1}}. \tag{19b}$$

Since the factor $\pi d_0^3/(128 l_0)$ in Eq. (19) is a constant and has the dimension of permeability, we get the dimensionless effective permeability of the composites,

$$K_{e,x}^+ = \frac{K_{e,x}}{\pi d_0^3/(128 l_0)} = (1+\psi_x)\tan\theta \frac{1-\gamma/(n\beta^4)}{1-[\gamma/(n\beta^4)]^{m+1}}, \tag{20a}$$

$$K_{e,y}^+ = \frac{K_{e,y}}{\pi d_0^3/(128 l_0)} = \frac{(1+\psi_y)n}{2\tan\theta} \frac{1-\gamma/(n\beta^4)}{1-[\gamma/(n\beta^4)]^{m+1}}. \tag{20b}$$

Substituting Eq. (20) into Eq. (11) yields

$$\vec{K}_e^+ = \begin{bmatrix} K_{e,x}^+ & 0 \\ 0 & K_{e,y}^+ \end{bmatrix} = \begin{bmatrix} (1+\psi_x)\tan\theta \dfrac{1-\gamma/(n\beta^4)}{1-[\gamma/(n\beta^4)]^{m+1}} & 0 \\ 0 & \dfrac{(1+\psi_y)n}{2\tan\theta} \dfrac{1-\gamma/(n\beta^4)}{1-[\gamma/(n\beta^4)]^{m+1}} \end{bmatrix}, \tag{21}$$

where $\vec{K}_e^+ = \frac{\vec{K}_e}{\pi d_0^3/(128 l_0)}$ is the dimensionless effective permeability tensor of the composite. Equation (21) presents the dimensionless total effective permeability tensor of composites with an embedded V-shaped fractal-like tree network after m iterations. This model is closely related to the structural parameters of the network, i.e., ψ, β, γ, θ, and m.

C. Compared to the traditional parallel channel net

In order to study the unique influence of the fractal-like tree networks on the channel-matrix composite system, we compare our model with the traditional parallel channel net under the same relative surface porosities ψ_x and ψ_y. To this end, we assume that there are n^{m+1} (n^{m+1} is also the total number of outlets in the fractal-like tree networks after m

iterations) parallel channels with the unified diameter d and tube length $b/2$ or a, embedded in the matrix material in the x or y direction. These parallel channels have the same total volume as the fractal-like networks.

The total volume of the parallel channels arranged in the x direction can be expressed as

$$V_x = n^{m+1}\pi d^2(b/2)/4 \tag{22}$$

and the total volume of the tree network is

$$V_t = \sum_{k=0}^{m} n^{k+1}\pi(d_k/2)^2 l_k = \frac{\pi d_0^2 l_0 n}{4}\frac{1-(n\beta^2\gamma)^{m+1}}{1-n\beta^2\gamma}. \tag{23}$$

Since the total volume of the parallel channel net and the tree network is equal, combining Eq. (22) and Eq. (23), we can obtain the diameter of a parallel cylinder

$$d^2 = \frac{d_0^2}{n^m \sin\theta}\frac{1-\gamma}{1-\gamma^{m+1}}\frac{1-(n\beta^2\gamma)^{m+1}}{1-n\beta^2\gamma}. \tag{24}$$

Under the fully developed laminar flow, the permeability of parallel channels is [24]

$$K = \frac{d^2}{32}. \tag{25}$$

Substituting Eq. (24) into Eq. (25) yields

$$K = \frac{d_0^2}{32n^m \sin\theta}\frac{1-\gamma}{1-\gamma^{m+1}}\frac{1-(n\beta^2\gamma)^{m+1}}{1-n\beta^2\gamma}. \tag{26}$$

Equation (26) describes the permeability for flow through parallel channels.

Since the matrix material has the permeability K_m, by utilizing Eq. (18) and Eq. (26), we can get the effective permeability of a composite with an embedded traditional parallel net (in the x direction)

$$K_{p,x} = \frac{d_0^2(1+\psi_y)}{32n^m \sin\theta}\frac{1-\gamma}{1-\gamma^{m+1}}\frac{1-(n\beta^2\gamma)^{m+1}}{1-n\beta^2\gamma}. \tag{27}$$

In Eq. (27), the factor $d_0^2/32$ is the permeability of a single cylinder at initial level 0, Eq. (27) can be thus expressed as the dimensionless form

$$K_{p,x}^{+} = \frac{K_{p,x}}{d_0^2/32} = \frac{(1+\psi_x)}{n^m \sin\theta}\frac{1-\gamma}{1-\gamma^{m+1}}\frac{1-(n\beta^2\gamma)^{m+1}}{1-n\beta^2\gamma}. \tag{28a}$$

Similarly, we can obtain the dimensionless effective permeability for a composite with an embedded traditional parallel net in the y direction as follows:

$$K_{p,y}^{+} = \frac{(1+\psi_y)}{n^m \cos\theta}\frac{1-\gamma}{1-\gamma^{m+1}}\frac{1-(n\beta^2\gamma)^{m+1}}{1-n\beta^2\gamma}. \tag{28b}$$

III. RESULTS AND DISCUSSIONS

In a composite with embedded fractal-like tree networks, both the matrix material and the microstructures of the networks determine the behavior of the composite.

Equation (20a) divided by Eq. (20b) yields

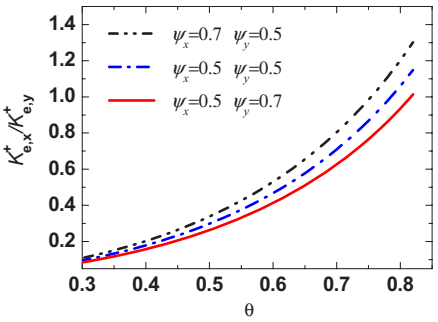

FIG. 3. (Color online) $K_{e,x}^{+}/K_{e,y}^{+}$ versus θ at different ψ_x and ψ_y.

$$K_{e,x}^{+}/K_{e,y}^{+} = \frac{2(1+\psi_x)\tan^2\theta}{n(1+\psi_y)}. \tag{29}$$

Equation (29) suggests that $K_{e,x}^{+}$ increases while $K_{e,y}^{+}$ decreases as branching angle θ increases in the range of $0-\pi/2$. When $\theta=45°$ and $\psi_x=\psi_y$ (i.e., the branching channels are isotropic growth, and the relative surface porosity is identical in the x and y direction), $K_{e,x}^{+}$ is equal to $K_{e,y}^{+}$. In this case, fluid homogeneously flows through the network-matrix composite. Moreover, the effective permeability increases with the increase of the relative surface porosity. Figure 3 clearly shows these features.

Figure 4 shows the dimensionless effective permeability $K_{e,y}^{+}$ versus the diameter ratio β at different γ. The results denote that the dimensionless effective permeability $K_{e,y}^{+}$ increases with the increase of diameter ratio β and decreases with the increase of length ratio γ. This is expected because a higher diameter ratio β implies the larger daughter branching channels, leading to the lower flow resistance and higher permeability. On the contrary, a higher length ratio γ means the longer branching channels, leading to the higher flow resistance and lower permeability. It is also surprisingly found from Fig. 4 that the dimensionless effective permeability $K_{e,y}^{+}$ scales as the diameter exponent by $K_{e,y}^{+}\sim\beta^{\alpha m}$ when $\beta<0.707$. From the figure we can get the approximate relation $\ln K_{e,y}^{+}\sim(m\ln\frac{n}{\gamma}+4m\ln\beta)$ as $n\beta^4/\gamma<1$ and $\beta<0.707$. This result means that the term $\ln K_{e,y}^{+}$ is directly proportional to the term $4m\ln\beta$, and which shows that the constant α is close to 4.

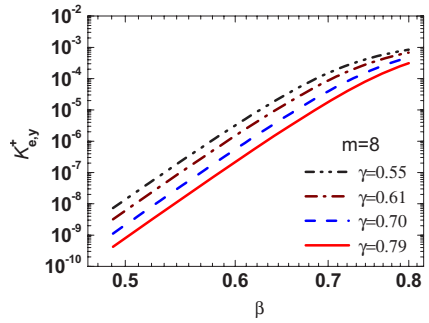

FIG. 4. (Color online) $K_{e,y}^{+}$ versus diameter ratios β at different length ratios γ when $\psi_y=0.65$, $\theta=0.58$.

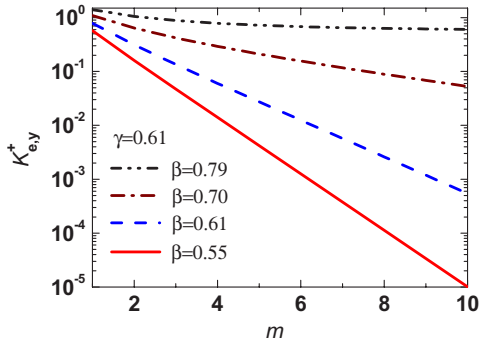

FIG. 5. (Color online) $K^+_{e,y}$ versus iterations m at different β when $\psi_y=0.65$, $\theta=0.58$, $\gamma=0.61$.

Figure 5 presents the dimensionless effective permeability $K^+_{e,y}$ versus iteration m under fixed γ and different β. From Fig. 5 we can find that the branch iteration number has significant effect on the effective permeability. When the iteration number m increases, the network becomes denser, and this will increase the flow resistance and lead to the lower permeability. Figure 5 also denotes that the higher the ratio β, the less the influence of iterations m on $K^+_{e,y}$ at the same length ratio γ (=0.61), the slope of the curve at $\beta=0.55$ is larger than that of the curve at $\beta=0.79$. Furthermore, the curve in Fig. 5 shows a scaling behavior between m and $K^+_{e,y}$. This can be explained that $K^+_{e,y}$ isproportional to the term $n\beta^4/\gamma$ when $m>1$ and $n\beta^4/\gamma<1$, and we have the approximate relation $\ln K^+_{e,y}/m \sim \ln(n\beta^4/\gamma)$. On the contrary, when $n\beta^4/\gamma>1$, $K^+_{e,y}$ is proportional to a constant and no scaling behavior exists.

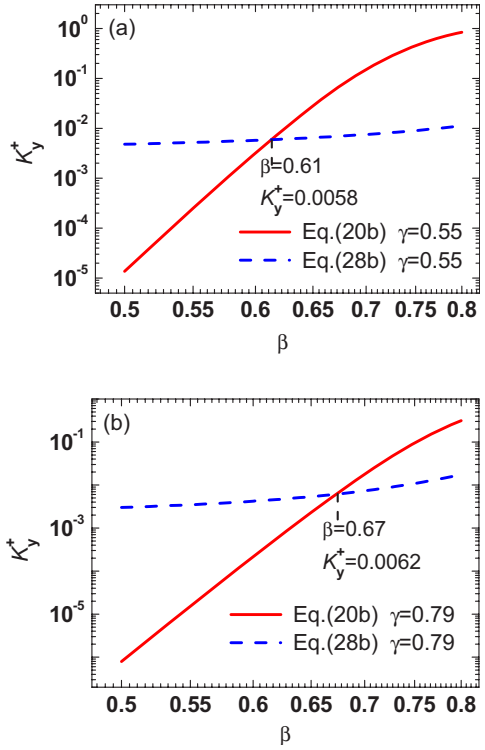

FIG. 6. (Color online) A comparison of effective permeability in the positive y direction versus β between different models at $\psi_y=0.65$, $m=8$, $\theta=0.58$.

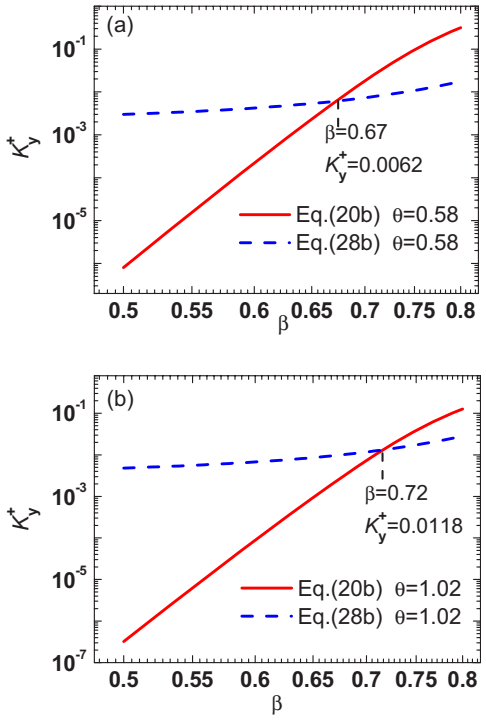

FIG. 7. (Color online) A comparison of effective permeability in the positive y direction versus β between different models at $\psi_y=0.65$, $m=8$, $\gamma=0.79$.

Figure 6 compares the dimensionless effective permeabilities in the positive y direction versus diameter ratio β between the two models at different values of γ. It is interestingly found that when $\beta>0.61$, the effective permeability $K^+_{e,y}$ is higher than $K^+_{p,y}$ at $\gamma=0.55$ in Fig. 6(a). The similar phenomenon is found in Fig. 6(b), i.e., the values of $K^+_{e,y}$ are higher than those of $K^+_{p,y}$ as $\beta>0.67$. This can be explained that the flow resistance of the branching channel networks is greater than the parallel channel networks at the less diameter ratio β. However, since the connectivity of branching channel networks exceeds the parallel channel networks, the flow resistances of the branching channel networks decrease as β increasing. This results in the effective permeability $K^+_{e,y}$ higher than $K^+_{p,y}$. Figure 6 also shows the rule about the value of diameter ratio β at the intersection point, which increases with the increase of the length ratio γ.

Figure 7 compares the dimensionless effective permeabilities in the positive y direction versus diameter ratio β between the two models at different branching angles θ. We can also find that the intersections of these curves change with branching angle changing. For example, see Fig. 7(a), when $\theta=0.58$ and $\beta>0.67$, the effective permeability $K^+_{e,y}$ is higher than $K^+_{p,y}$. Furthermore, we find the values of β at the intersection points increase with the increase of branching angle θ.

Figure 8 compares the dimensionless effective permeabilities in the positive y direction versus diameter ratio β between the two models when iterations m change. From Fig. 8 it can be seen again that the permeability $K^+_{e,y}$ is higher than $K^+_{p,y}$ when diameter ratio β is higher than a certain value, e.g., $\beta>0.73$ for iteration $m=4$ in Fig. 8(a) and

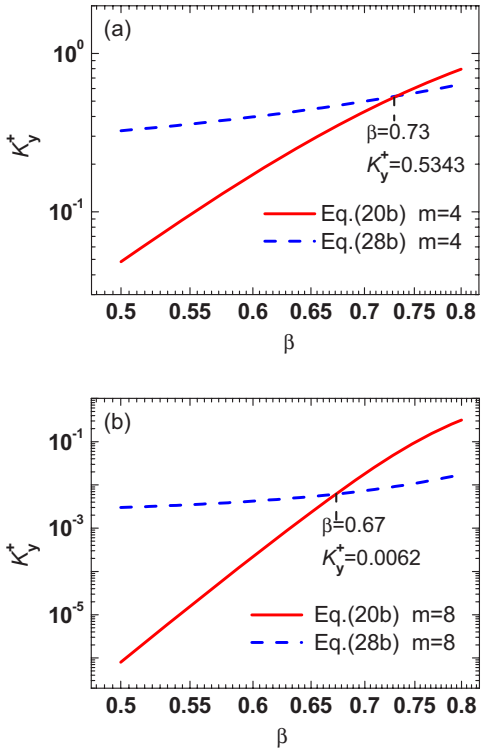

FIG. 8. (Color online) A comparison of effective permeability in the positive y direction versus β between different models at ψ_y=0.65, θ=0.58, γ=0.79.

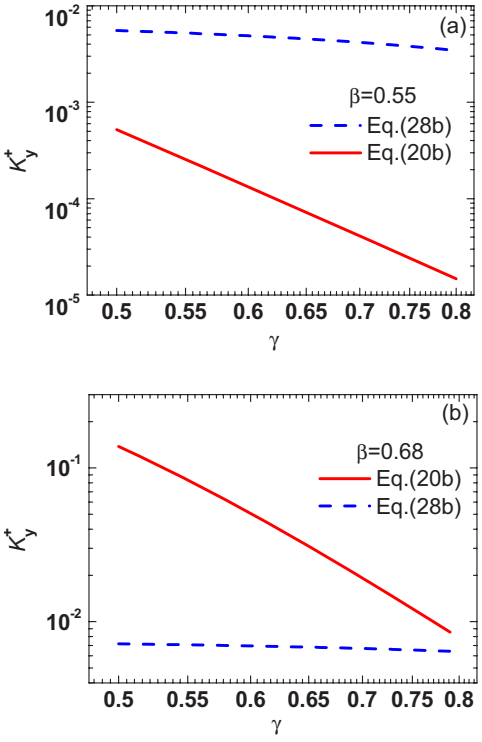

FIG. 9. (Color online) A comparison of the effective permeabilities in the positive y direction versus γ between different models at m=8, θ=0.58, ψ_y=0.65.

$\beta > 0.67$ for iteration m=8 in Fig. 8(b). Figure 8 also reveals that the value of β at the intersecting point decreases with the increase of iteration m. These results may be important for design of the proper matrix material and the structural parameters of the branching networks.

Figure 9 compares the dimensionless effective permeabilities in the positive y direction between different models. It is found that effective permeability $K_{e,y}^+$ is lower than $K_{p,y}^+$ at β=0.55 in Fig. 9(a). But when diameter ratio β is assigned a larger value, for example, β=0.68 in Fig. 9(b), the permeability $K_{e,y}^+$ is remarkably higher than $K_{p,y}^+$. The higher value of β, a much higher permeability $K_{e,y}^+$ than $K_{p,y}^+$ is found.

Figure 10 presents the effective permeabilities in the positive y direction versus iterations m between different models. As expected, when length ratio γ and diameter ratio β are at lower values (e.g., $\gamma=\beta$=0.55), the dimensionless effective permeability $K_{e,y}^+$ is lower than $K_{p,y}^+$, see Fig. 10(a). While γ and β are assigned the larger values [e.g., $\gamma=\beta$=0.68 in Fig. 10(b)], the permeability $K_{e,y}^+$ is higher than $K_{p,y}^+$. From Figs. 9 and 10 we see that the dimensionless effective permeability $K_{e,y}^+$ may be much higher than $K_{p,y}^+$ under properly chosen microstructural parameters of the networks.

Similarly, we can find the behaviors of the effective permeability $K_{e,x}^+$ in the positive x direction.

IV. CONCLUDING REMARKS

In this paper, we have studied the effective permeabilities of composites with embedded self-similar fractal-like tree networks. We have found that the effective permeability is closely related to the microstructures of the branching networks: the effective permeability increases with the increase of the diameter ratio β or the relative surface porosity be-

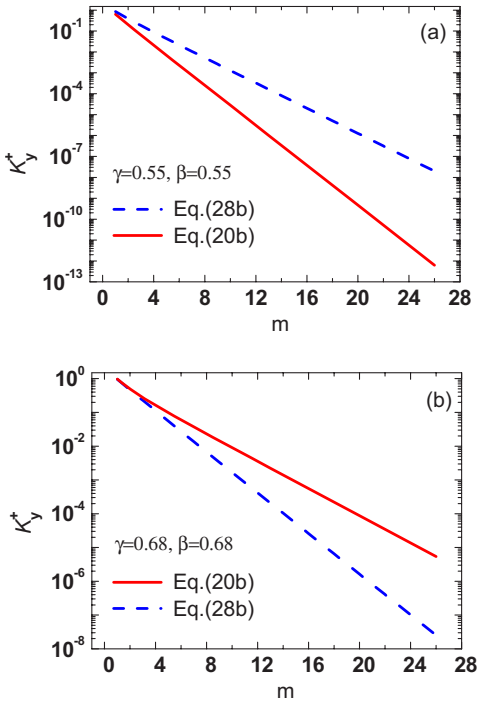

FIG. 10. (Color online) A comparison of the effective permeability in the positive y direction versus m between different models at θ=0.58, ψ_y=0.65.

tween matrix and tree networks; and the effective permeability decreases with the increase of length ratio γ as well as iteration m. It is surprisingly found that when diameter ratio $\beta < 0.707$, the dimensionless effective permeability of composites scales as the diameter exponent by $K_{e,y}^{+} \sim \beta^{\alpha m}$, with $\alpha \approx 4$. And it is also found that when $m > 1$ and $n\beta^4/\gamma < 1$, the effective permeability $K_{e,y}^{+}$ scales as the iteration m, $\ln K_{e,y}^{+}/m \sim \ln(n\beta^4/\gamma)$. The results have shown that at the properly chosen length ratios γ, the fractal-like tree networks can significantly increase the effective permeability of composites compared to the parallel channel nets. The effective permeability of composites with embedded fractal-like tree networks may be higher than that of composites embedded with traditional parallel nets when β is larger than a certain value, depending on the branching angle, relative surface porosity, length ratio, and iteration m.

Our results suggest that properly choosing the structure parameters of the networks is urgent in design of composites and cooling systems, and in analysis of networks.

ACKNOWLEDGMENTS

This work was supported by the National Natural Science Foundation of China through Grant No. 10572052.

[1] D. R. Morse, J. H. Lawton, J. H. Dodson, and M. M. Williamson, Nature (London) **314**, 731 (1985).
[2] A. H. Fitter and T. R. Strickland, Funct. Ecol. **6**, 632 (1992).
[3] H. Kitaoka, R. Takaki, and B. Suki, J. Appl. Physiol. **87**, 2207 (1999).
[4] G. B. West, J. H. Brown, and B. J. Enquist, Nature (London) **400**, 664 (1999).
[5] S. Bohn, B. Andreotti, S. Douady, J. Munzinger, and Y. Couder, Phys. Rev. E **65**, 061914 (2002).
[6] B. Berkowitz, Adv. Water Resour. **25**, 861 (2002).
[7] B. M. Yu and P. Cheng, J. Thermophys. Heat Transfer **16**, 22 (2002).
[8] D. Tondeur and L. A. Luo, Chem. Eng. Sci. **59**, 1799 (2004).
[9] I. Leifer and J. Boles, Mar. Pet. Geol. **22**, 551 (2005).
[10] W. R. Gutierrez, Phys. Rev. E **66**, 041906 (2002).
[11] S. N. Dorogovtsev and J. F. F. Mendes, *Evolution of Networks: From Biological Nets to the Internet and the WWW* (Oxford University Press, Oxford, 2003).
[12] K. I. Goh, G. Salvi, B. Kahng, and D. Kim, Phys. Rev. Lett. **96**, 018701 (2006).
[13] A. Bejan, Int. J. Heat Mass Transfer **40**, 799 (1997).
[14] A. Bejan, *Advanced Engineering Thermodynamics*, 2nd ed. (Wiley, New York, 1997), Chap. 13.
[15] A. Bejan, *Shape and Structure from Engineering to Nature* (Cambridge University Press, Cambridge, UK, 2000).
[16] M. Neagu and A. Bejan, J. Appl. Phys. **86**, 1136 (1999).
[17] A. Bejan, L. A. O. Rocha, and S. Lorente, Int. J. Therm. Sci. **39**, 949 (2000).
[18] W. Wechsatol, S. Lorente, and A. Bejan, Int. J. Heat Mass Transfer **45**, 4911 (2002).
[19] B. M. Yu and B. W. Li, Phys. Rev. E **73**, 066302 (2006).
[20] P. Xu, B. M. Yu, Y. J. Feng, and Y. J. Liu, Physica A **369**, 884 (2006).
[21] P. Xu, B. M. Yu, Y. J. Feng, and M. Q. Zou, Phys. Fluids **18**, 078103 (2006).
[22] B. B. Mandelbrot, *The Fractal Geometry of Nature* (Freeman, New York, 1982).
[23] M. J. Ronayne and S. M. Gorelick, Phys. Rev. E **73**, 026305 (2006).
[24] A. E. Scheidegger, *The Physics of Flow Through Porous Media* (University of Toronto, Ontario, 1974), Chap. 4.
[25] B. M. Yu and L. J. Lee, Polym. Compos. **21**, 660 (2000).